polymer papers

Lamellar structure in a thin polymer blend film

M. Geoghegan, R. A. L. Jones* and R. S. Payne†
Cavendish Laboratory, University of Cambridge, Cambridge CB3 0HE, UK

and P. Sakellariou
ICI Paints, Research Department, Wexham Road, Slough, Berkshire SL5 2DS, UK

and A. S. Clough
Department of Physics, University of Surrey, Guildford, Surrey GU2 5XH, UK

and J. Penfold
Rutherford Appleton Laboratory, Chilton, Didcot, Oxfordshire OX11 0QX, UK
(Received 27 July 1993; revised 25 October 1993)

We have fully characterized the three-dimensional morphology of thin films of mixtures of polystyrene and polybutadiene cast from a toluene solution, using nuclear reaction analysis, neutron reflectometry and transmission electron microscopy. Polystyrene-rich phases wet both the air and substrate interfaces and are separated by a polybutadiene-rich phase; these layers are very well defined and the interfaces between them are sharp (down to <20 Å). Within the polybutadiene-rich central layer, lateral phase separation is also evident, with polystyrene-rich domains of oblate spheroidal shape. Under certain circumstances thin polystyrene-rich layers exist within the polybutadiene-rich phase. We discuss possible mechanisms for this unusual morphology in terms of surface effects on the mechanism of phase separation in the ternary polymer–solvent system from which the films are cast.

(Keywords: polystyrene–polybutadiene blend; thin film; lamellar structure)

INTRODUCTION

Composition profiles near the surface of polymer mixtures are profoundly affected by the presence of that surface. The surface of a miscible polymer blend, at equilibrium, will be enriched in the component of lower surface energy. This kind of surface segregation phenomenon is common to all binary mixtures, but the effects are particularly marked for polymer mixtures; the entropy of mixing is very weak in polymer blends, so even small surface-energy differences lead to large surface segregation effects. The natural length scale is set by the chain dimensions, and so segregation may persist to quite large depths. These factors should lead to surface effects being important for two-phase polymer mixtures. The equilibrium situation will usually be that one phase completely wets the surface; what is much less clear is whether, or how, this equilibrium situation is reached. If a quench is made into the metastable phase region of the phase diagram, a wetting layer may grow in a uniform manner[1]. At least for shallow quenches, this mechanism should be favoured over bulk nucleation and growth, as no activation energy is involved. The more usual situation, in which the mixture is quenched into the unstable part of the phase diagram, is more complicated and is not yet fully understood, with a complicated interplay between bulk- and surface-driven phase separation. In the bulk one expects phase separation to take place by spinodal decomposition, in which random composition fluctuations are amplified with strong selection of fluctuations of a certain wavelength. This results in a structure consisting of a superposition of composition waves of roughly constant wavelength but random phase and direction. The presence of a surface may fix the phase and direction of the composition waves, resulting in surface-directed spinodal decomposition; here a composition wave propagates perpendicularly from the surface into the bulk until coherence is lost due to thermal fluctuations, and the morphology becomes characteristic of the bulk[2–5]. These surface-directed composition waves are also vulnerable to the effect of coarsening owing to their high interfacial energy. The energy cost in supporting a series of waves perpendicular to the surface becomes too great and the pattern breaks up away from the surface.

Experimental study of the effect of surfaces and interfaces on films of immiscible polymer mixtures is increasing with the availability of techniques capable of probing polymer films. Surface analysis techniques have shown that the surface composition of solvent-cast films of immiscible polymers may not be the same as the bulk composition[6]. Light scattering has been used to examine phase separation in polystyrene–poly(vinyl methyl ether)[7] and poly(methyl methacrylate) and poly(vinyl acetate)[8] films. The direct-space depth-profiling techniques of

* To whom correspondence should be addressed
† On leave from ICI Materials, Wilton Research Centre, Wilton, Middlesborough, Cleveland TS6 8JE, UK. Present address: Zeneca Pharmaceuticals, Macclesfield, Cheshire SK10 2NA, UK

0032-3861/94/10/2019-09

forward recoil spectrometry (FReS) and nuclear reaction analysis (NRA) have been used to good effect in various studies. Isotopic blend films of poly(ethylene–propylene) quenched into the two-phase region of the phase diagram were studied by FReS and NRA[9,10]. The deuterated component adsorbed to the vacuum interface, whilst the hydrogenated polymer adsorbed to the silicon substrate interface. A surface-directed spinodal decomposition morphology was observed with spinodal waves propagating from the front and back of the sample and then interfering when the waves met. Bruder and Brenn[11] also observed surface-directed spinodal decomposition in a film of a blend of deuterated polystyrene and poly(styrene-*co*-4-bromostyrene) (PBrS) using time-of-flight FReS and optical microscopy. The PBrS adsorbed onto a chromium-plated substrate, forming a bilayer structure, but lateral phase separation prevented any depth structure in the film prepared on the oxide layer of a silicon wafer. Steiner *et al.*[12] used NRA to observe isotopic bilayers of random copolymers of ethylene and ethyl-ethylene reach their coexistence compositions. After reaching the coexisting compositions, a wetting layer of one of the copolymers at the air surface was reported. There is a very strong link between wetting and bulk phase separation, and this is discussed by Guenoun *et al.* in a study of a methanol–cyclohexane mixture[13].

The ability to tailor the surface of a polymer film from an initially uniform film has great potential in a variety of areas such as coatings, paints and barrier films. In this paper we report the formation of a lamellar morphology in an immiscible polymer blend after solvent casting. An understanding of the statistical mechanics of polymer surfaces may enable coatings to be prepared in a single-stage process rather than by present methods that involve techniques such as coextrusion or various surface treatments.

We report here the characterization of a striking morphology in a thin film of an immiscible polymer blend, which we conjecture is produced by a surface-driven phase separation process. In order to achieve as complete a characterization of the morphology as possible, we have used a number of different techniques. In order to measure a composition–depth profile, averaged over a large area of the film, we used helium-3 nuclear reaction analysis. The depth resolution of this technique in the configuration that we used is of order 400 Å, so to characterize internal interfaces with better resolution we used neutron reflectometry (NR), which with good contrast can resolve to better than 10 Å. In order to gain information about lateral structure in the film we used transmission electron microscopy (TEM), imaging both in the plane of the film and on thin ultramicrotomed sections cut perpendicular to the film.

We have studied films of blends of polystyrene (PS) and polybutadiene (PB). These polymers are known to be immiscible for all but the lowest molecular weights, with a large, positive Flory–Huggins interaction parameter[14,15]. The ternary phase diagram for this system is shown in *Figure 1*. There is conflict as to whether the interaction parameter is independent of the effect of deuterating one of the components. The results of Atkin *et al.*[17] show a significant isotope effect on deuteration of the polybutadiene. Small-angle neutron scattering experiments comparing PS–PB blends in which each component in turn is deuterated also reveal an isotope effect[18]. In re-examining this question using light scattering, Lin *et al.*[19] find no discernible isotope effect when the aromatic hydrogen atoms on the polystyrene are replaced by deuterium. They ensured that the two polystyrene isotopes were closely matched in size and structure by using similar preparation procedures. In any event, the isotope effect would only be significant for a blend more miscible than the one described here.

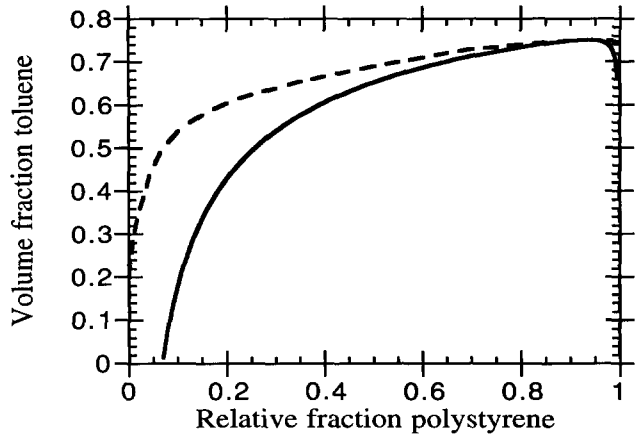

Figure 1 The ternary phase diagram for a blend of polystyrene (of molecular weight 5050) and polybutadiene (540000) at 300 K. The broken curve details the spinodal and the full curve the binodal. The abscissa details the volume fraction of polymer that is polystyrene. The Flory–Huggins interaction parameter used is that determined by Roe and Zin[14], $\chi_{AB}=(53.434/T)(1.573+0.09\phi-0.0021T)$, where T is the absolute temperature and ϕ is the polystyrene volume fraction. The lattice parameter, defined by toluene, is 5.6065 Å. χ_{AB} is multiplied by the total polymer volume fraction to account for shielding, an approximation only valid at low solvent concentrations. The PS–toluene and PB–toluene interaction parameters are taken as 0.436 and 0.465 respectively[16]

EXPERIMENTAL

For nuclear reaction analysis and neutron reflectometry we used fully deuterated polystyrene (d-PS) of molecular weight (M_w) 4550; for electron microscopy we also used normal polystyrene (h-PS) of a similar molecular weight, 5050. In both cases polybutadiene of molecular weight 540000 was used. All materials were prepared by anionic polymerization, and had polydispersity indices of 1.03 for the polystyrene and 1.06 for the polybutadiene. The polystyrene was purchased from Polymer Laboratories and the polybutadiene was a gift from L. J. Fetters (Exxon). We used densities of 1.132 g cm^{-3} (d-PS), 1.053 g cm^{-3} (h-PS) and 0.895 g cm^{-3} (PB) in our calculations. For NRA and NR studies thin films, typically ~4000 Å thick, were spun-cast from toluene (typically ~3% polymer by weight in solution) onto silicon substrates (from which the native oxide layer had not been removed). A wide range of PS concentrations was studied (from 9.5% to 77.5% by volume), all below the calculated critical volume fraction, which is estimated to be 0.935. The critical volume fraction is calculated to be 0.930 when h-PS is used (see *Figure 1*). These values should be treated with caution; a light scattering study of the PS–PB–toluene system noted poor agreement between the theoretical and experimental critical compositions[16].

The technique of NRA[20] was used at the Device Fabrication Facility at the University of Surrey to determine direct-space deuterium depth profiles in the films. A Van de Graaff generator is used to provide a beam of typically 700 keV $^3He^+$ ions. This penetrates the

sample and reacts with the deuterons to produce high-energy protons. The energy of the emergent protons is measured, providing direct information about the deuterated polymer concentration as a function of depth in the sample. NRA profiles are shown for three samples in *Figure 2*. These reveal d-PS-rich layers both at the surface and at the interface with the silicon, separated by a layer rich in PB. The observed profile is the convolution of the actual profile and a Gaussian resolution function.

The CRISP neutron reflectometer[21] at the spallation neutron source, ISIS, was used for the neutron reflection experiments. Because protons and deuterons have very different scattering lengths, excellent contrast is provided between the deuterated polystyrene and polybutadiene used in these experiments. The effective refractive index encountered by the neutrons on traversing the sample is linearly related to the concentration of d-PS; thus measurements of the reflection coefficient as a function of neutron wavelength can be interpreted to yield the d-PS concentration–depth profile[22,23]. Reflectivity profiles, R, as a function of the perpendicular component of neutron momentum, k, for five samples are shown in *Figure 3*. The period of the fringes is too large for them to be characteristic of the total film thickness; instead it derives from lamellar structure within the films and is due to interference between the front and back of the internal layers. The characteristic thickness, d, of the layers is given by $d=\pi/\Delta k$, where Δk is the fringe thickness, and the sharpness of the fringes is related to the sharpness of the interfaces between the layers. To analyse the data more quantitatively we assume a model profile consisting of deuterated-polystyrene-rich layers at the surface and the substrate, separated by a polybutadiene-rich layer. The composition profile, $\phi(z)$, across the first interface (between the surface layer of d-PS and the PB-rich layer) is given by a complementary error function of the form:

$$\phi(z)=\phi_2+\frac{\phi_1-\phi_2}{\mathrm{erfc}(d/\sigma)}\,\mathrm{erfc}\left(\frac{z+d}{\sigma}\right)$$

where ϕ_1 and ϕ_2 are the d-PS volume fractions at the surface and in the middle layer, respectively, d is an offset and σ is the interfacial width. The interface between the PB-rich layer and the d-PS-rich layer at the substrate is given by a similar (error function) profile. The experimental resolution was folded in with the model. Best-fit model parameters were obtained by least-squares fitting using a downhill simplex algorithm. A more detailed description of NR data analysis is given by Jones *et al.*[24]. It is well known that fits obtained from neutron reflectivity data may not be unique owing to the loss of phase information. This is not a problem in these experiments because we are able to use models whose general form and initial parameters are derived from the lower-resolution but direct-space technique of nuclear reaction analysis.

Electron microscopy investigations were performed using a JEOL 2000EX transmission electron microscope (in the Cavendish Laboratory) or a Phillips CM30 (at ICI Wilton). It proved to be impossible to float the films off the silicon substrates that we used for NRA and NR experiments, so the samples were spun onto glass microscope slides and floated onto the surface of distilled water, from which they were picked up on TEM grids. They were then vapour-stained with OsO_4 at ~55°C for about 2 h. In order to check that using a glass substrate rather than a silicon one did not substantially alter the morphology, NRA was performed on a 44.5% d-PS film prepared on a glass substrate, floated off onto a water surface and picked up on a silicon substrate. The resulting depth profile was indistinguishable from that produced

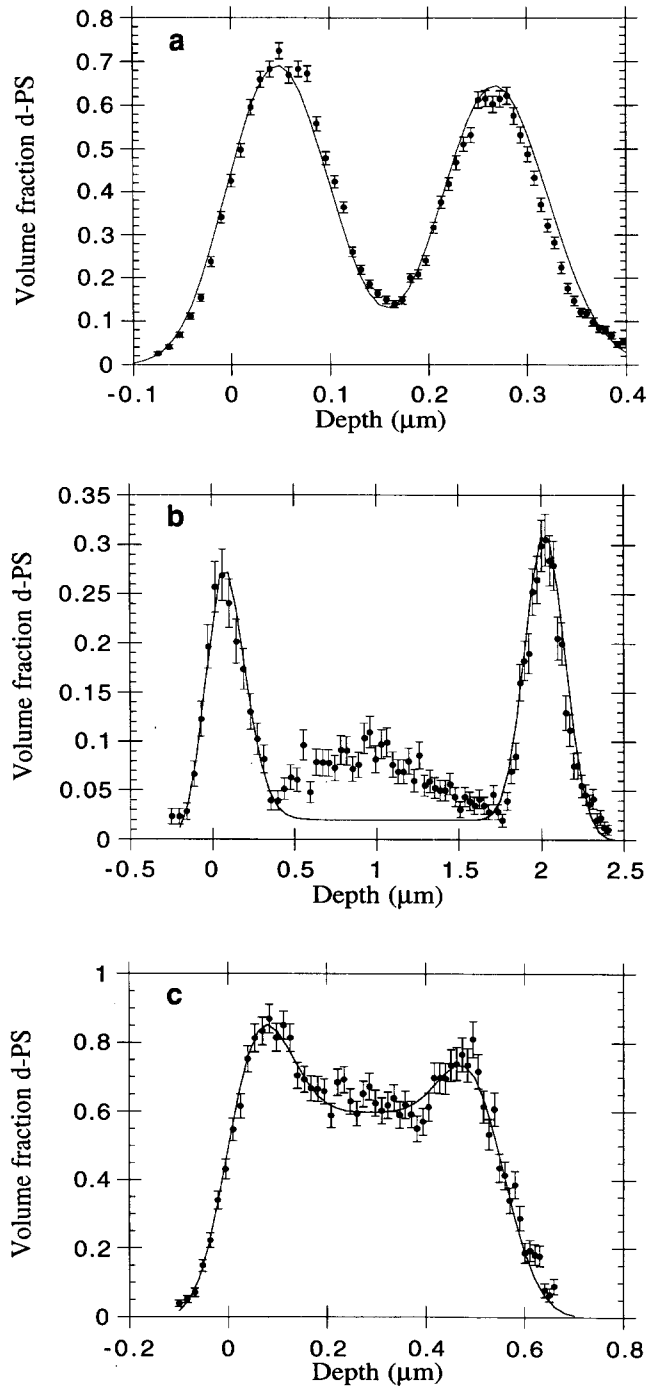

Figure 2 (a) An NRA profile for a sample (0.31 μm thick) containing 53.7% by volume d-PS (full circles). The error bars are due to random statistical errors only. The result of the fit to the neutron reflectivity data is also shown convolved with the resolution function of the NRA experiment (full curve). This convolution masks the sharpness of the interfaces. (b) NRA data for a film (2.1 μm thick) containing 12.4% by volume d-PS. Note that the surface layer is less enriched in d-PS than the substrate (the surface excess is 340 Å at the air interface and 900 Å at the substrate). The full curve is the best fit to the front and back peaks. No attempt was made to fit the laterally phase-separated region in the centre of the sample. (c) NRA data for a 0.55 μm thick film containing 76.0% by volume d-PS. The full curve is the result of a three-layer fit

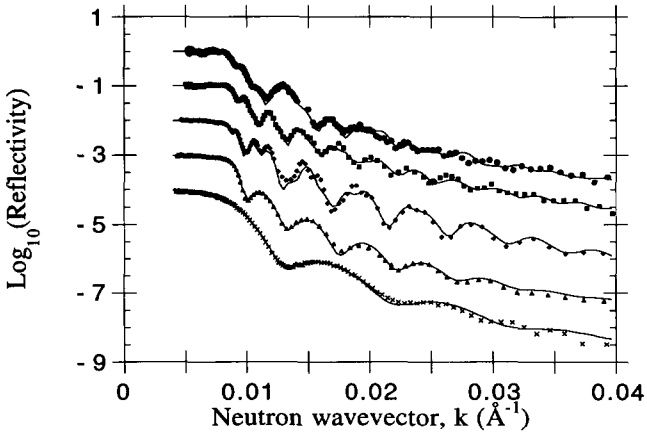

Figure 3 Reflectivity, R, data against the perpendicular component of neutron momentum, k (related to neutron wavelength, λ, by $k=(2\pi/\lambda)\sin\theta$, where θ is the angle of incidence of the neutron beam to the sample) for films containing 9.5 (×), 17.4 (▲), 44.5 (◆), 53.7 (■) and 75.5% (●) d-PS by volume. These data are staggered by a decade in reflectivity each for clarity. The quality of the fits varies, with values of χ^2 of 3.5, 26.8, 214, 5.5 and 3.8 respectively

by direct spinning onto silicon. To obtain cross-sectional views of the films, pieces of film were picked up from a water bath on loops of nylon fibre and stained with OsO_4 vapour. They were then embedded in LR white resin (an acrylic-based embedding resin) and cut into thin sections with an LKB Ultratome III ultramicrotome and a diamond knife. Other sections were made using Araldite epoxy resin in order to see if the interaction between the resin and the sample could be reduced. The sectioned samples are usually somewhat thicker than the corresponding films from which planar views were taken, as thicker films are more self-supporting when picked up on the nylon fibre. However, thinner films were necessary for planar views, as those thicker than about 4000 Å become opaque to the electron beam.

RESULTS

The NRA data clearly reveal a trilayer morphology, examples of which are shown in *Figure 2*. For the sample containing 76.0% d-PS by volume, this morphology is less obvious, since the large amount of d-PS present in the central region prohibits a dramatic layered structure. NRA shows that less material has segregated to the front than to the back in the 12.4% sample.

The NRA data provided a starting point for the NR fits. An example of the result to a fit to NR data is shown overlaying the NRA data of *Figure 2a*, where the samples were cast from the same solution. A series of NR data and best fits using the trilayer morphology are supplied in *Figure 3*. We find good agreement between data and fits for such models, where the interfaces are represented by error functions with characteristic widths of between 10 and 120 Å. The larger widths occur in the thicker films rich in polybutadiene. Sharper interfaces occur in films with more polystyrene. An ambiguity that does persist is that it is impossible to ascribe widths to the front or back interface independently when these widths are approximately the same size. To illustrate this, consider the reflectivity profile from the 53.7% d-PS film; after the data points corresponding to total reflection have been removed, the χ^2 value for the fit increases from 7.8 to only 9.7 if the two interfacial roughnesses (originally 49 Å at the front interface and 10 Å at the back) are interchanged. It is, however, possible to distinguish the effects of broadening of the internal interfaces from roughness at the surface since surface roughness causes a drop in reflectivity and has little effect on fringe width. Another complication is that, owing to lateral phase separation, significant small-angle scattering may be taking place and a large amount of off-specular reflection is observed. In the 75.5% d-PS sample it was not possible using the trilayer morphology to obtain a fit that both satisfied the NRA data and conserved volume of material. In most cases this is not obvious as the middle, PB-rich, layer does not provide a significantly reflecting surface and so minor alterations to the composition of this layer can be performed without significantly changing the quality of the fit. (The thickness of this middle layer affects the 'beating' of the outer two layers.) In the case of the 75.5% d-PS sample, however, the middle layer should still be rich in d-PS. It is believed, therefore, that small-angle scattering from d-PS domains in the middle layer accounts for this discrepancy.

The values of χ^2 for the reflectivity data are shown in the caption to *Figure 3*. The varying quality of the fits needs some explanation. In the 44.5% sample, the reflectivity close to the critical edge (the point at which total reflection occurs at lower wavenumbers) is not matched very well by the fit. This is the largest contributing factor to the value of χ^2 of 214 since the statistics are excellent in this region. The probable cause of this discrepancy is loss of neutrons due to scattering. Incoherent scattering of neutrons from hydrogen[24] is accounted for in our fitting procedure by the inclusion of complex scattering length densities, but small-angle scattering due to lateral composition inhomogeneities is not. Any weakness in the fit around the critical edge does not affect the interfacial width and layer thickness obtained from the fits and the influence on the volume fractions obtained for the layers is minimal. The most significant systematic error is the uncertainty in knowing the angle of the neutron beam to the sample. This causes an inaccurate value of k, and we estimate that this results in an uncertainty of $<5\%$ in the interfacial widths and layer thicknesses. We have made an investigation of the effect of putting into the model profile a thin middle d-PS-rich layer as suggested by some of the electron micrographs (*Figure 5*), but we found that this did not improve the fits.

Taken together, the NRA and NR data give a good composition–depth profile through the film. In addition, the strong off-specular scattering seen in the NR experiments indicates the possibility of phase separation in the plane of the film, but this was visible in an optical microscope only in those samples with about 75% d-PS. Electron microscopy was therefore necessary. *Figure 4* shows TEM micrographs of a film containing 14.4%, 45.6% and 76.9% polystyrene by volume. All micrographs reveal PS-rich domains, all of which, except those in the 79.7% sample, were previously invisible. The differing size scales of domains on the 14.4% sample are likely to be due to domains coalescing. There are many domains of approximately 0.25 μm in diameter in the 45.6% sample. This sample (*Figure 4b*) also shows clear cracks. The origin of these cracks is at present unknown, but we speculate that they are formed by the PS layers fracturing as they pass through the glass transition. Polybutadiene has seeped into these cracks, explaining

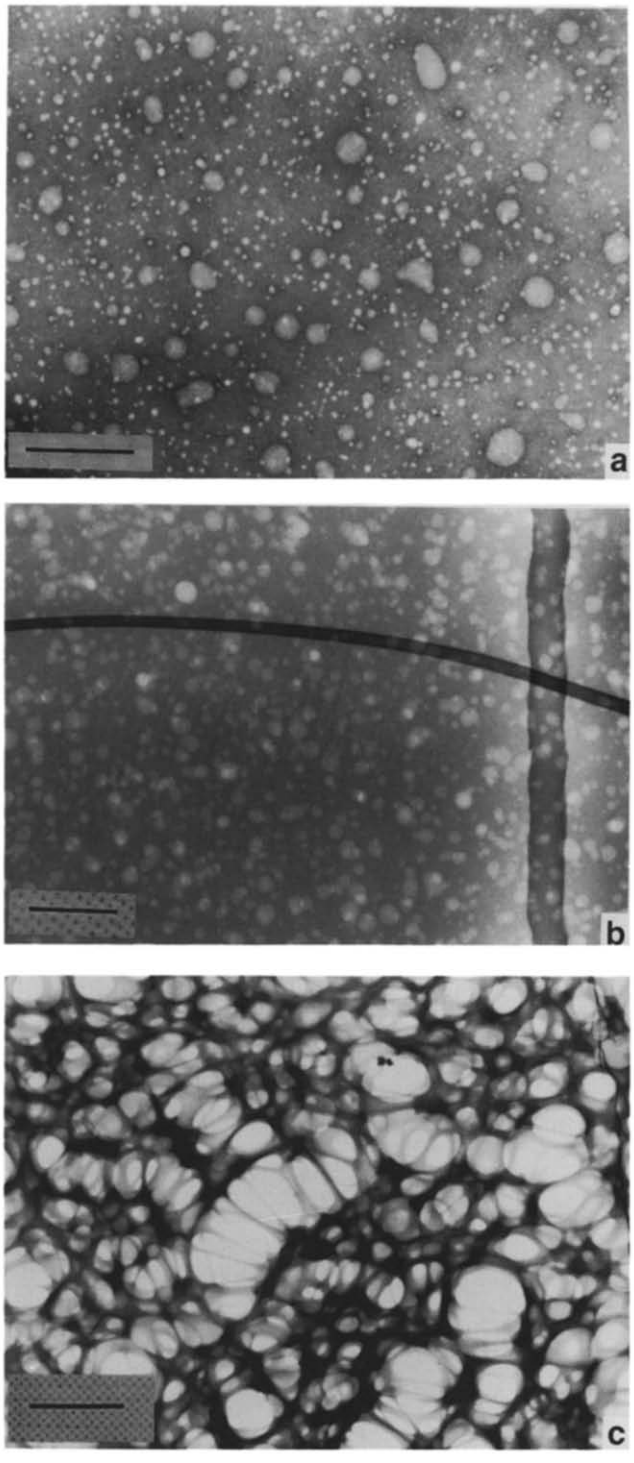

Figure 4 TEM micrographs of samples containing (a) 14.4%, (b) 45.6% and (c) 76.9% h-PS by volume. The scale bar is 1 μm. The dark regions correspond to the electron-dense OsO_4-stained PB-rich regions. Polystyrene-rich domains are clearly visible in all samples, but in the 76.9% sample the size of the phase-separated regions (up to 1 μm) is considerably greater than in the other samples. The micrograph for the 45.6% sample also illustrates cracks in the film

their dark nature. The increase in contrast where two cracks intersect (*Figure 4b*) is evidence for cracks appearing on both sides of the film. Electron energy-loss spectroscopy experiments indicate that the film is almost constant in thickness across these cracks.

Conventional TEM does not tell us at what depth these domains are in the film and so cross-sectioned samples were prepared by ultramicrotomy. Micrographs of such sections are shown in *Figure 5*. The interface between the polystyrene-rich surface layers and the embedding medium cannot be resolved because the low-molecular-weight PS is easily dissolved in the resin. A separate experimental test on the PS alone confirmed that it did readily dissolve in the resin. Without the PS-rich surface layers, the section thickness is less than the total film thickness. Not all sections follow a straight path; the film in *Figure 5b* is particularly curved. This is

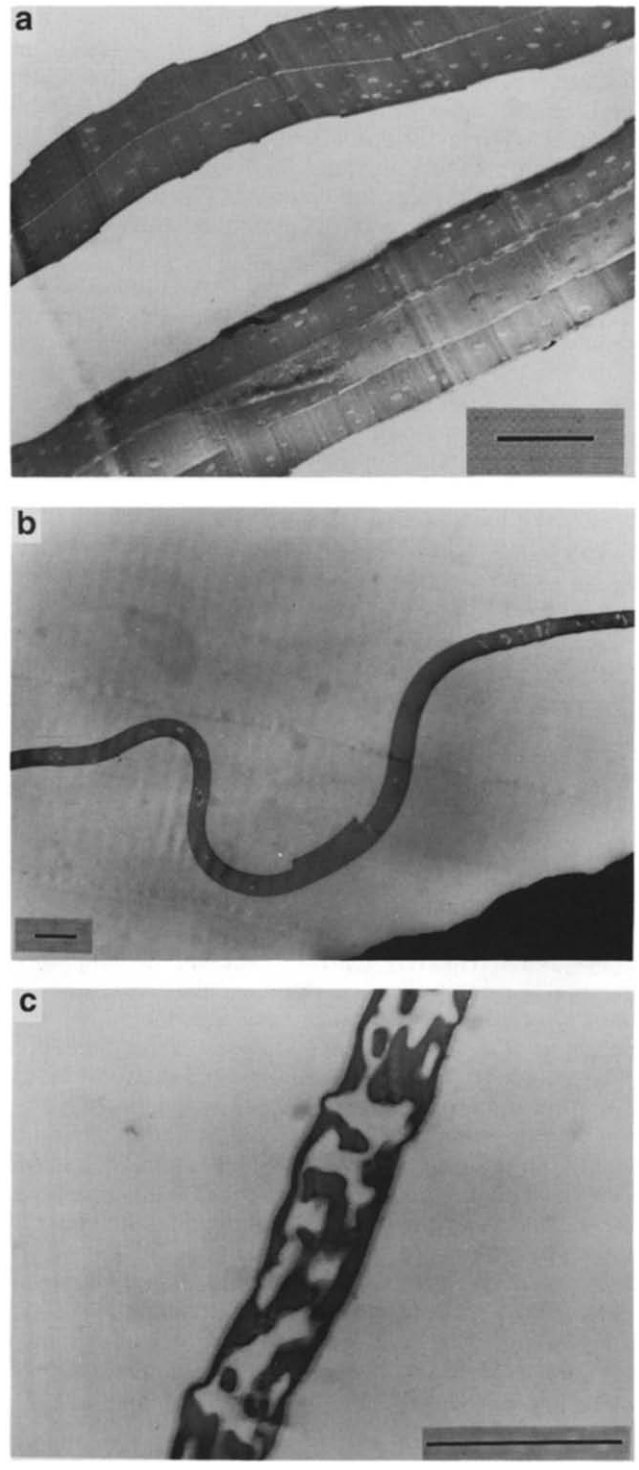

Figure 5 TEM micrographs of sections of samples containing (a) 13.0%, (b) 45.6% and (c) 77.5% h-PS by volume. The scale bar is 1 μm. The thickness of each film is not necessarily equal to the thickness of its section, as the section may have been cut at less than 90°. We are confident that this is not the case except for that of the film containing 45.6% h-PS, which appears to be very much thicker than would be expected

due to the effect of picking up such a delicate film from water and later placing it in a capsule into which resin is then introduced. Two sections are visible in the 13.0% sample (*Figure 5a*). This is because the film has been folded around the nylon line when picked up from water. Despite the fact that the two sections have a different number of layers, they are from the same film. In the 45.6% film (*Figure 5b*) the region where the PB fills a crack (see *Figure 4b*) is evident. As well as the PS-rich domains, there are regions where PB-rich domains are surrounded by PS-rich shells. The cause of these phase-inverted domains is unknown, but there are further isolated PB-rich domains in a polystyrene matrix in the micrograph of the 77.5% section (*Figure 5c*). Here the morphology is a little different in that the size of the phase-separated regions is much greater than in the other sections. The shape of the domains (*Figures 5a* and *5b*) can be seen to be oblate spheroidal when taken in conjunction with the planar views. The domains in the 45.6% sample are all central in the micrograph; this was characteristic of all the micrographs taken of sections of films with a similar PS concentration. Most interesting is the existence of the two thin layers of polystyrene in the 13.0% sample.

Thus by a combination of techniques we are able to build up a reasonably complete three-dimensional picture of the morphology of thin films of an immiscible polymer blend. At the surface of the films is a well defined layer rich in polystyrene. The central part of the films is made up by a thicker polybutadiene-rich layer (in some cases containing further thin polystyrene-rich layers). This is separated from the polystyrene-rich layer by an interface whose width can be of order ~20 Å. Within the central polybutadiene-rich layer, polystyrene-rich domains are formed of oblate spheroidal shape, with aspect ratios usually between 1.5 and 3. Next to the silicon substrate is another polystyrene-rich layer, of similar thickness to the first, again very well defined and separated from the central layer by an interface width of order 20 Å. Both polystyrene-rich layers are fractured on a relatively coarse scale, resulting in a pattern of cracks approximately 1 μm wide on the surface and 200 nm on the substrate. The domains are relatively central in the 45.6% samples. In the 13.0% sample they are more evenly distributed but there is (are) one (or sometimes two) uniform polystyrene-rich layer(s) within this film.

Although we have made no systematic study of the evolution of these morphologies over long periods of time, we have repeated the neutron reflectometry measurements on one sample, consisting of 44.5% d-PS, two months after the original experiment. This revealed that the d-PS-rich layers had each increased in thickness by some 50 Å, but that the interfacial widths between the layers remained essentially unchanged. Repeated experiments (six months apart) on a sample with 75.5% d-PS showed that the film had lost its original morphology completely, the competition provided by the bulk growth destroying the lamellar morphology in a manner similar to that described by Bruder and Brenn[11].

DISCUSSION

These complicated and striking morphologies are evidently the result of a complex interplay of equilibrium effects, such as wetting, and kinetic effects resulting from the way in which the samples are prepared. As a result, a quantitative explanation of the way in which the morphologies arise would be difficult. However, drawing on the growing understanding of the effects of surfaces on phase transitions in polymer mixtures, we can suggest the factors that may govern the production of such lamellar structures in thin films. In this system phase separation is initiated, not by a temperature jump, but by evaporation of the toluene during the spin-casting process, as illustrated by the schematic ternary phase diagram in *Figure 6*. As the toluene (which is a neutrally good solvent for both polymers) evaporates, its effect as a diluent diminishes until a polymer concentration is reached at which polymer–polymer interactions become significant[25]. At this point phase separation occurs. If we were dealing with a bulk sample, we would expect this to result in the formation of a pattern of roughly spherical domains of the minority phase, which coarsen with time. However, in a thin film we must be aware of the possibility that phase separation takes place by means of the growth, at the surface and substrate, of wetting layers of the phase of lower surface energy. In our case the growth of these wetting layers will be interrupted, because as toluene is progressively removed from the system the d-PS-rich layers at the surface and the substrate will eventually become glassy. The NR data reveal that the surface layer contains polystyrene volume fractions of between 0.8 and 0.9. This is very low for such an immiscible system; one would not expect the polybutadiene to be this soluble in the polystyrene. The upper coexistence volume fraction was negligibly different from unity when estimated using the value of χ_{AB} determined by Roe and Zin[14] at room temperature (see *Figure 1*). The low surface and substrate polystyrene volume fractions are attributable to the system becoming glassy before all the solvent has evaporated. This glass transition provides another complication to understanding the mechanisms of the formation of the lamellar morphology.

It is worth while considering the films separately in a more detailed approach. We divide this into three sections dealing with samples containing around 15%, 50% and 75% polystyrene, respectively, to compare with the available micrographs.

(i) *15% polystyrene.* In the most off-critical blend, that containing 15% polystyrene, NR and NRA data

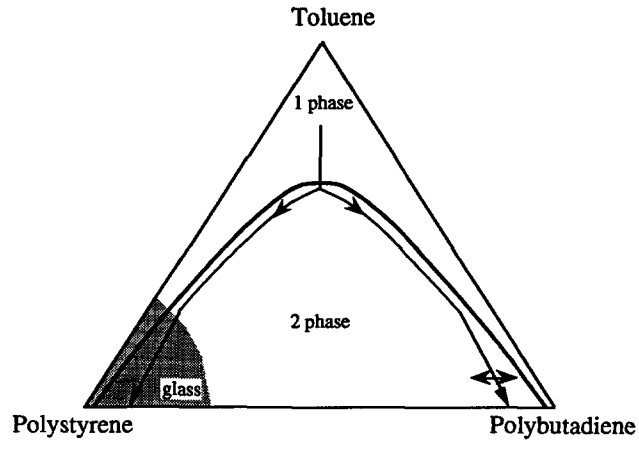

Figure 6 Schematic ternary phase diagram showing the evolution of the film during the casting process. The bold full curve is the coexistence curve and the arrowed line indicates the separate paths followed by the bulk and surface layers after the coexistence curve is crossed

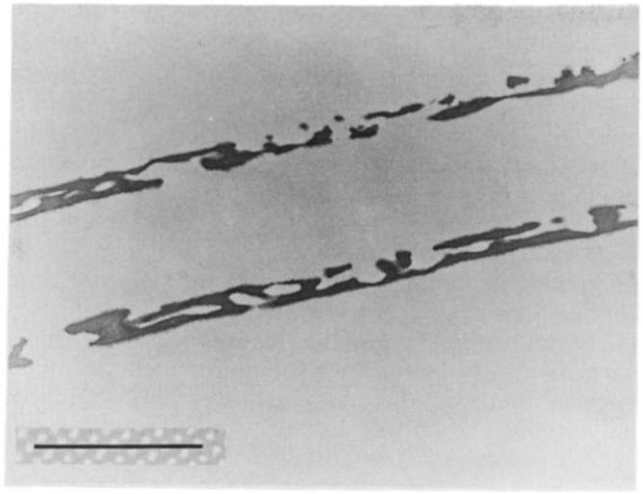

Figure 7 Two sections of a film containing 76.9% h-PS by volume. The scale bar is 1 μm. This film is thinner than the corresponding film in *Figure 5c* and we can see regions where the polystyrene-rich surface layers are connected

indicate that the surface layer is not as enriched in polystyrene as the substrate layer. We speculate that the surface is not as enriched as the substrate owing to a solvent concentration gradient in the spin-casting process. The solvent concentration will always be lower at the surface than at the substrate in the spin-casting process. The craters that are visible in the section (*Figure 5a*) are of an unknown origin. It is likely that these craters are filled with polystyrene that has not managed to fully wet the interface since the phase is undersaturated[26] in the ternary system. These craters may be the surface droplets predicted by Marko[5] for shallow quenches. It is unlikely that there is a PS layer on top of these craters, since the reflectometry experiments would then be expected to reveal a higher surface volume fraction than if there was a fully formed wetting layer. Values of ϕ of 0.63 and 0.40 were obtained for the d-PS layer at the air interface in the 9.5% and 17.4% samples, respectively. The internal polystyrene-rich layers are probably due to a surface-directed spinodal decomposition process. The region of the film where only one line exists is about 1 μm thick, with the line situated in the middle. Curiously, the region with two lines is 1.5 μm thick. The 9.5% d-PS NR sample was about 0.5 μm thick, and the fit to the data could not be improved by including a d-PS-rich middle layer. In the case of the thicker films the spinodal waves from the front and back of the sample interfere constructively, forming these layers. There is no evidence here that the spinodal waves are damped out by thermal fluctuations. The domains are presumably formed independently of the surface-triggered phase separation. The oblate spheroidal shape of the domains may possibly have been induced by surface fields, as in bulk phase separation these would be expected to be spherical. The lamellar structure may favour coalescence parallel to the lamellae, leading to oblate spheroids, similar to the argument proposed by Guenoun *et al.* to explain the shape of the non-wetting cyclohexane phase in their experiment[13]. Marko has observed oblate domains[27] in his cell dynamical model[5,10] when applied to off-critical quenches.

(ii) *50% polystyrene.* The films containing 50% polystyrene have a much simpler morphology than those described above. In this case there seems to be no domain formation other than in the centre of the film. These domains may be the remains of a line rich in polystyrene that has broken up in the coarsening process. Such a line may never have fully formed, as the spacing between domains is very large. In this case we suggest that, although a surface-directed spinodal decomposition mechanism is likely to be responsible for the depth profile, the interfacial energy required to form a middle layer proved to be too great. There are some phase-inverted domains visible in the section micrograph (*Figure 5b*). In these a PB-rich domain is contained within a PS-rich shell. The cause of these is not known.

(iii) *75% polystyrene.* The 75% polystyrene system is different in that the lateral phase separation is clearly visible in an optical microscope. The section shows a morphology in which there are not only isolated polystyrene-rich domains but also an interconnected structure. In other (thinner) sections there are regions where the polystyrene cuts right through the film (*Figure 7*). A possible explanation for such broken intermediate layers is that the film is smaller than the characteristic spinodal decomposition wavelength. This phenomenon has been postulated by Krausch *et al.*[10] in their work on interference between spinodal waves travelling from both the surface and substrate. Krausch *et al.* used cell dynamical simulations for a system in which the hydrogenous polymer preferentially adsorbed to the substrate and the deuterated component to the vacuum surface. The wavelength at which the lamellar morphology breaks down is thus 1.5 times the spinodal wavelength. In our system the lamellar morphology should hold for films thicker than the spinodal wavelength. For this explanation to hold, the spinodal wavelength for our system would have to be between 2000 and 5000 Å. Unfortunately, we are not able independently to estimate this wavelength, as we do not know the solvent composition at which phase separation commenced. Light scattering measurements could in the future elucidate this point.

The interfacial width between the surface layers and the polybutadiene-rich region has been determined by the reflectometry experiments to be lower than 20 Å. Theoretical prediction of the interfacial width for such an asymmetric immiscible system is difficult. The original Helfand–Tagami theory[28–30] was modified by Helfand and Sapse[31] to allow for polymers with differing densities and statistical segment lengths. Further modifications to the theory have been made by Broseta *et al.*[32] to account for finite-molecular-weight and polydispersity effects. For monodisperse systems of incompatible polymers, the following interfacial width, D, is derived:

$$D=\frac{2a}{(6\chi_{AB}\pi)^{1/2}}\left[1-2\left(\frac{1}{N_A\chi_{AB}}+\frac{1}{N_B\chi_{AB}}\right)\ln 2\right]^{-1/2}$$

where a is the statistical segment length (if σ_A and σ_B are the segment lengths of PS and PB, respectively, then $a^2=\sigma_A^2(1-\phi)+\sigma_B^2\phi$), N_A and N_B are the chain lengths and χ_{AB} is the Flory–Huggins interaction parameter. The factor $\pi^{1/2}$ converts the interfacial width from a hyperbolic tangent width, as defined by Helfand and Tagami, to that of an error function. In this case (h-PS/PB) an interfacial width of 8 Å is obtained at 300 K for a volume fraction $\phi=0.5$ using the value of χ_{AB} obtained by Roe and Zin[14]. The theory is meant to be applied to polymers with comparable molecular weights, as higher-order

terms in $N\chi_{AB}$ have been neglected, but the correction for our system is small. Caution should be exercised since the result of 8 Å may be inapplicable to square gradient theory, which requires the interfacial width to be smoothly varying on the length scale of a monomer unit. We should also note that capillary waves, which contribute to the interface width[33], are not taken into account in the above analysis. With this in mind, the result is in good agreement with the smallest interfacial width that we measured: 10 Å for the interface between the substrate layer of d-PS and the PB-rich central region in the 53.7% d-PS film. To our knowledge, there is little literature on the polystyrene–polybutadiene interface except for pendant drop measurements of the PS–PB interfacial tension[34]. Work in progress on bilayers of PB and a d-PS/h-PS blend[35] has revealed, with neutron reflectometry, an 18 Å (error function) width after annealing at 175°C.

One might be surprised at the PS wetting the substrate and not the PB, particularly given that the work of Hasegawa and Hashimoto on polystyrene and polyisoprene block copolymers reveals that the polyisoprene segregates to the air surface[36]. In another study, the addition of a few butadiene groups to a d-PS chain and terminated with trimethylsilane significantly improved d-PS adsorption onto silicon substrates[24]. The d-PS wetting the surface should be understood in the context of the polymer molecular weights. NRA performed on a blend containing 44.2% d-PS with molecular weights of 53 000 for both d-PS and PB showed that the air interface was enriched in PB. This is consistent with the generally accepted molecular-weight dependence of the surface energy, $E = A - k/M_w^{2/3}$, where A and k are constants. It must also be remembered that the wetting is in a ternary system and that the surface energy of the phases (as opposed to the individual components) is the critical parameter. We note that there appears to be a transition between incomplete wetting of the surface by a PS-rich layer for $\sim 15\%$ samples to complete wetting for $\sim 50\%$ samples. This may be connected to the plating transition (which is of kinetic origin) proposed by Marko[5], whereby, for shallow quenches, droplets are found at the surface, but for deeper quenches a wetting layer is found, even when equilibrium favours partial wetting.

Recent theoretical work has emphasized that *any* factor that breaks translational symmetry can lead to anisotropic phase separation[37]. In addition to the effects of surface-energy differences, there are two other possible causes of symmetry breaking that may have an effect in our system. The first possibility is that shear in the spin-casting process leads to elongation of the polymer molecules, possibly leading to asymmetric phase separation. Experimentally, it is known that shear inhibits phase separation in a semidilute solution of PS–PB in dioctyl phthalate[38]. To test for any effect of shear, we also prepared films (containing 44.7% d-PS by volume) by solvent casting without spinning, and found using NRA that the surface was enriched in d-PS. We also drew a film (45.1% d-PS) from a toluene solution at constant speed; NRA revealed this to be a trilayer structure and TEM revealed a similar morphology to that previously described. The second cause of symmetry breaking is the effect of a gradient in solvent composition with depth during the casting process. In films with only a small d-PS concentration (9.5% and 17.4%) the air interface is significantly less enriched in d-PS than the substrate interface. The greater solvent concentration at the substrate allows more time for the d-PS-rich layer to form at the substrate compared with that at the surface. In the case of these films, cracks are not visible at the surface, implying that the top layer is not glassy. Reflectivity analysis also reveals that the surface roughness of this top layer is comparatively greater than for those with greater d-PS concentrations (~ 35 Å as compared to ~ 10 Å). This is not unexpected for a non-glassy or phase-separated surface layer. Surface roughness has a very different effect on reflectivity data than does interfacial roughness; the latter tends to wash out fringes whereas the former lowers the reflectivity. In other systems, in which there is a greater concentration of polystyrene, the surface and substrate layers contain approximately equal compositions of polystyrene and are also about the same thickness. Here the gradient in solvent composition appears not to be significant and the system has reached equilibrium. A glance at the schematic phase diagram (*Figure 6*) will help to understand this; the quench into the two-phase region occurs at a lower solvent concentration for films with $\sim 15\%$ polystyrene. Less time is available for the structure to form in this case than in one in which phase separation commences at a much higher concentration of solvent.

CONCLUSIONS

In conclusion, we have characterized the morphology of thin films of an immiscible polymer blend produced by spin-casting from a common solvent. A striking lamellar morphology, with extremely well defined layers of the different phases, is revealed. While we are not in a position quantitatively to predict the appearance of such morphologies, we believe them to be due to surface effects on the mechanisms of phase separation. We have provided a qualitative explanation in the context of surface-induced phase separation in a ternary system. Our work has been compared to theoretical models and comparisons have been drawn with other systems. In view of the importance of thin polymer films for coatings, membranes and barrier films, such effects may have potential applications.

ACKNOWLEDGEMENTS

MG is grateful to the SERC and to ICI plc for support in the form of an SERC CASE award with ICI Wilton. Additional support was provided through the Colloid Technology Program, jointly funded by the Department of Trade and Industry, Schlumberger Cambridge Research, ICI plc and Unilever plc. This work has benefited from useful discussions with Dr J. F. Marko and Professor D. T. Grubb (Cornell University), J. Genzer and Dr R. J. Composto (University of Pennsylvania) and Drs P. J. Mills and S. Rostami (ICI Wilton). The assistance of Dr A. Burgess in the early stage of this work is acknowledged. The following have been a great help in the acquisition of neutron reflection data: C. Shackleton, C. J. Clarke and Drs T. Nicolai, S. Whineray and A. Eaglesham. Preliminary TEM was performed by Dr A. E. Dray.

REFERENCES

1 Sullivan, D. E. and Telo da Gama, M. M. in 'Fluid Interfacial Phenomena' (Ed. C. A. Croxton), Wiley, Chichester, 1986, p. 45
2 Ball, R. C. and Essery, R. L. H. *J. Phys.: Condens. Matter* 1990, **2**, 10303
3 Brown, G. and Chakrabarti, A. *Phys. Rev.* (*A*) 1992, **46**, 4829
4 Puri, S. and Binder, K. *Phys. Rev.* (*A*) 1992, **46**, 4487
5 Marko, J. F. *Phys. Rev.* (*E*) 1993, **48**, 2861
6 Gardella, J. A. *Appl. Surf. Sci.* 1988, **31**, 72
7 Reich, S. and Cohen, Y. *J. Polym. Sci., Polym. Phys. Edn.* 1981, **19**, 1255
8 Nesterov, A., Horichko, V. and Lipatov, Y. *Makromol. Chem., Rapid Commun.* 1991, **12**, 571
9 Jones, R. A. L., Norton, L. J., Kramer, E. J., Bates, F. S. and Wiltzius, P. *Phys. Rev. Lett.* 1991, **66**, 1326
10 Krausch, G., Dai, C.-A., Kramer, E. J., Marko, J. F. and Bates, F. S. *Macromolecules* 1993, **26**, 5566
11 Bruder, F. and Brenn, R. *Phys. Rev. Lett.* 1992, **69**, 624
12 Steiner, U., Klein, J., Eiser, E., Budkowski, A. and Fetters, L. J. *Science* 1992, **258**, 1126
13 Guenoun, P., Beysons, D. and Robert, M. *Phys. Rev. Lett.* 1990, **65**, 2406
14 Roe, R.-J. and Zin, W.-C. *Macromolecules* 1980, **13**, 1221
15 Ronca, G. and Russell, T. P. *Macromolecules* 1985, **18**, 665
16 Hashimoto, T., Sasaki, K. and Kawai, H. *Macromolecules* 1984, **17**, 2812
17 Atkin, E. L., Kleintjens, L. A., Koningsveld, R. and Fetters, L. J. *Makromol. Chem.* 1984, **185**, 377
18 Tomlins, P. E. and Higgins, J. S. *Macromolecules* 1988, **21**, 425
19 Lin, J.-L., Rigby, D. and Roe, R.-J. *Macromolecules* 1985, **18**, 1609
20 Payne, R. S., Clough, A. S., Murphy, P. and Mills, P. J. *Nucl. Instrum. Meth.* (*B*) 1989, **42**, 130
21 Penfold, J., Ward, R. C. and Williams, W. G. *J. Phys.* (*E*) 1987, **20**, 1411
22 Penfold, J. and Thomas, R. K. *J. Phys.: Condens. Matter* 1990, **2**, 1369
23 Russell, T. P. *Mater. Sci. Rep.* 1990, **5**, 171
24 Jones, R. A. L., Norton, L. J., Shull, K. R., Kramer, E. J., Felcher, G. P., Karim, A. and Fetters, L. J. *Macromolecules* 1992, **25**, 2359
25 Narasimhan, V., Huang, R. Y. M. and Burns, C. M. *J. Appl. Polym. Sci.* 1989, **37**, 1909
26 Cahn, J. W. *J. Chem. Phys.* 1977, **66**, 3667
27 Marko, J. F., private communication, 1993
28 Helfand, E. and Tagami, Y. *J. Polym. Sci., Polym. Phys. Edn.* 1971, **9**, 741
29 Helfand, E. and Tagami, Y. *J. Chem. Phys.* 1971, **56**, 3592
30 Helfand, E. and Tagami, Y. *J. Chem. Phys.* 1972, **57**, 1812
31 Helfand, E. and Sapse, A. M. *J. Chem. Phys.* 1975, **62**, 1327
32 Broseta, D., Fredrickson, G. H., Helfand, E. and Leibler, L. *Macromolecules* 1990, **23**, 132
33 Fredrickson, G. H. in 'Physics of Polymer Surfaces and Interfaces' (Ed. I. C. Sanchez), Butterworth-Heinemann, Boston, 1992, p. 1
34 Anastasiadis, S. H., Gancarz, I. and Koberstein, J. T. *Macromolecules* 1988, **21**, 2980
35 Genzer, J., private communication, 1993
36 Hasegawa, H. and Hashimoto, T. *Macromolecules* 1985, **18**, 589
37 Essery, R. L. H. *PhD Thesis*, University of Cambridge, 1992
38 Takebe, T., Fujioka, K., Sawaoka, R. and Hashimoto, T. *J. Chem. Phys.* 1990, **93**, 5271